Resource Allocation for CoMP in Cellular Networks with Base Station Switching

Yoghitha Ramamoorthi and Abhinav Kumar,
Department of Electrical Engineering, Indian Institute of Technology Hyderabad, Telangana, 502285 India.
Email: {ee15resch02007, abhinavkumar}@iith.ac.in

arXiv:1609.02286v2 [cs.NI] 24 Jan 2017

***Abstract*—Base station switching (BSS) can results in significant reduction in energy consumption of cellular networks during low traffic conditions. We show that the coverage loss due to BSS can be compensated via coordinated multi-point (CoMP) based transmission in a cluster of base stations. For a BSS with CoMP based system, we propose various BSS patterns to achieve suitable trade-offs between energy savings and throughput. We formulate the CoMP resource allocation and $\alpha-$Fair user scheduling as a joint optimization problem. We derive the optimal time fraction and user scheduling for this problem and use it to formulate a simplified BSS with CoMP optimization problem. A heuristic that solves this problem is presented. Through extensive simulations, we show that suitable trade-offs among energy, coverage, and rate can be achieved by appropriately selecting the BSS pattern, CoMP cluster, and rate threshold.**

***Index Terms*—α-Fair throughput, base station switching (BSS), cellular networks, coordinated multi-point (CoMP) transmission, downlink, energy.**

I. Introduction

The significant increase in demand of data has led to deployment of a huge number of base stations (BSs) in cellular networks. The BSs consume nearly 80% of the total energy consumed in cellular networks [1], out of which 70% is consumed by power amplifiers, processing circuits, and air conditioners [2]. These BSs are typically designed and deployed for peak user demands. However, it has been shown in [3] that the user demand varies with time resulting in underutilized BSs and switching off some BSs during low user demand results in significant energy savings. Further, in [4], it has been shown that around 2% of global Carbon emission is from cellular networks. Thus, base station switching (BSS) during low user demand is advantageous from both economical and ecological reasons, i.e., reduction in energy consumption and Carbon footprint of the network, respectively.

In [3], a dynamic BSS strategy has been studied based on the spatial and temporal traces of real-time downlink traffic. It has been shown in [5] that upto 30% energy can be saved in a cellular network through BSS. In [6], the energy and throughput trade-offs for a given coverage have been evaluated. To overcome the coverage constraint in BSS, infrastructure sharing through multi-operator service level agreements has been proposed in [7]. A small cell based approach for BSS has been presented in [8] and [9]. Further, a dynamic BSS strategy based on hybrid energy supplies has been presented in [10].

A promising approach for increasing edge users performance (equivalently coverage) in cellular networks is coordinated multi-point (CoMP) based transmission and reception. Joint transmission (JT), and coordinated scheduling/beamforming are the two variants of CoMP which have been discussed in [11]. In this work, we consider only CoMP with JT for our analysis and use CoMP with JT interchangeably with CoMP throughout the text. A coverage probability based analysis of CoMP systems using stochastic geometry has been derived in [12]. Further, in [13], it has been shown through analysis that CoMP can improve coverage upto 17%. The resource allocation for CoMP has been presented in [14]. A new scheduling policy for two tier CoMP network with one macro-cell and multiple small cells is proposed in [15]. However, BSS with CoMP has recently been studied.

A stochastic geometry based analysis of outage and coverage probabilities for BSS with CoMP has been performed in [16]. In [17], the outage probability for a hexagonal grid model of BSS with CoMP in terms of signal-to-noise-ratio (SNR) has been derived. The energy efficiency analysis of BSS with CoMP, under the constraint that only one BS can be switched off, has been obtained in [18]. The fundamental trade-off between energy efficiency and spectral efficiency for BSS with CoMP taking backhaul power consumption into account has been discussed in [19]. The performance of BSS with CoMP taking only uplink into consideration has been recently investigated in [20]. Enlarged coverage and improved energy savings for BSS with CoMP has been presented in [21]. However, the trade-off with respect to users' throughput has not been considered in [21]. A recent study on JT variant of CoMP has been presented in [22] that shows improvements in throughput at the cost of outage probability. The trade-off between energy, coverage, and throughput for BSS with CoMP has not been jointly studied in the literature. Further, suitable resource allocation schemes for BSS with CoMP that achieve these trade-offs are required. This is the motivation of this work.

The contributions of this paper are as follows.

- Various possible CoMP configurations and BSS patterns are proposed and compared.
- The joint BSS and CoMP for cellular networks is formulated as an optimization problem that is shown to be a mixed integer non-linear program (MINLP).
- A decomposed problem of joint resource allocation and user scheduling for CoMP is formulated as an optimization problem. Given an $\alpha-$Fair scheduler, optimal user scheduling for CoMP and non-CoMP users, and the optimal resource allocation for a CoMP cluster is derived.

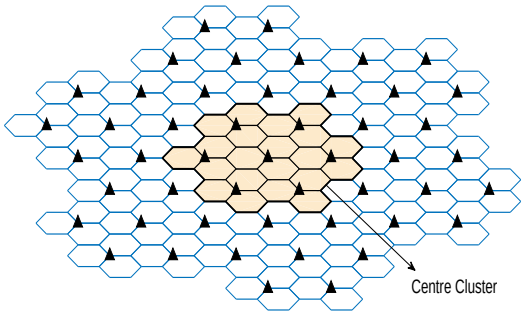

Fig. 1: Benchmark system with the wraparound layout around center cluster (reuse factor 1).

Note that the derived CoMP results in this work are independent of the BSs' topology.

- The optimal CoMP solutions are used to re-frame a BSS with CoMP optimization problem that is relatively solvable.
- A dynamic heuristic is proposed that solves the optimization problem for an energy efficient point of operation without compromising on coverage or user rates.
- The proposed results along with various CoMP configurations and BSS patterns are used to achieve the various trade-offs among energy, coverage, and throughput.

The organization of the paper is as follows. The system model is described in Section II. The Joint BSS and CoMP problem is formulated and analyzed in Section III. In Section IV, resource allocation and user scheduling for the decomposed CoMP problem is presented as an optimization problem along with the derivation of the optimal solutions. The simplified BSS with CoMP optimization problem is re-framed in Section V. A novel heuristic that solves the BSS with CoMP problem is described in Section VI. Extensive numerical results are presented in Section VII. Some concluding remarks along with possible future works are discussed in Section VIII.

II. SYSTEM MODEL

A. Benchmark System

We consider a homogeneous OFDMA based LTE cellular network as shown in Fig. 1. The set of BSs and corresponding sectors in the network are denoted by $\mathcal{B} = \{1, 2, ..., B\}$ and $\mathcal{S} = \{1, 2, ..., S\}$, respectively. Note that the BSs are represented by triangles in Fig. 1. The hexagons represent the corresponding sectors of a BS such that each BS has three sectors. Without any loss of generality, we assume that the set of sectors is ordered with the set of BSs. Hence, any BS $b \in \mathcal{B}$ corresponds to the sectors $3b-2$, $3b-1$, and $3b$, in the set $\mathcal{S}$. For example, in Fig. 2a, BS 4 corresponds to sectors 10, 11, and 12. We denote the set of users in the system by $\mathcal{U} = \{1, 2, ..., U\}$. We consider that the users are uniformly distributed in the system for a given user density μ. Let $\mathcal{M} = \{1, 2, ..., M\}$ denote the set of subchannels available in the network. We consider a reuse factor of 1. Hence, a total of M subchannels are allotted to each sector in $\mathcal{S}$. A comprehensive list of mathematical notations used in this paper is presented in Table I. Next, we present the channel model considered in this paper.

TABLE I: Mathematical notations.

C_i	CoMP configurations
G_s	Antenna directivity gain
$h^m_{u,s}$	Channel gain at user u from sector s on the subchannel m
P^m_s	Power allocated per subchannel m by sector s
$r_{u,s}$	link rate of user u from sector s
α	Fairness parameter for the α-Fair scheduler
$\beta_{u,s}$	Time fraction allocated for user u by a sector s
$\beta_{u,k}$	Time fraction allocated for user u by a virtual cluster k
$\eta(.)$	Spectral efficiency in $bits/symbol$
Γ_d	CoMP SINR threshold in dB
$\gamma^m_{u,s}$	Received SINR of user u from a sector s
$\gamma^m_{u,k}$	Received SINR of user u from a virtual cluster k
λ_u	Downlink rate for a user u
μ	User density per km^2
$\mathcal{B}$	Set of BSs with order B
$\mathcal{B}_q$	Set of BSs in the cluster q
$\mathcal{E}$	Percentage energy saved
$\mathcal{K}_q$	Set of virtual clusters in cluster q
$\mathcal{M}$	Set of subchannels with order M
$\mathcal{Q}$	Set of clusters with order Q
R	Rate threshold
$\mathcal{S}$	Set of sectors with order S
$\mathcal{S}_k$	Set of sectors in virtual cluster k
$\mathcal{T}_\alpha$	α-Fair throughput
$\mathcal{U}$	Set of users
$\mathcal{U}_k$	Set of users in virtual cluster k
$\mathcal{V}_q$	Set of users in the cluster q
$\mathcal{W}_q$	Set of sectors in cluster q
$\mathcal{Z}_{a1/a2}$	BSS pattern where $a1$ out of $a2$ BSs are switched off
$\mathbb{U}$	Utility function for α-Fair scheduler
$\lvert.\rvert$	Cardinality of a set
$\lceil.\rceil$	Ceil the input to smallest following integer

B. Channel Model

We consider a time division duplex (TDD) system. For mathematical brevity, we assume a frequency flat channel model and focus on the downlink. However, a similar analysis is possible for a frequency selective channel and uplink. The downlink signal-to-interference-plus-noise ratio (SINR) of a user u from a sector s, denoted by $\gamma^m_{u,s}$, on a subchannel m is given as

$$\gamma^m_{u,s} = \frac{P^m_s h^m_{u,s}}{\sum\limits_{\substack{\hat{s}\neq s \\ \hat{s}\in\mathcal{S}}} P^m_{\hat{s}} h^m_{u,\hat{s}} + \sigma^2}, \tag{1}$$

where, P^m_s is the power allocated to the subchannel m by the sector s, $\sum\limits_{\substack{\hat{s}\neq s \\ \hat{s}\in\mathcal{S}}} P^m_s h^m_{u,\hat{s}}$ is the interference on the subchannel m, σ^2 is the noise power, and $h^m_{u,s}$ denotes the channel gain between the sector s and the user u. The channel gain is given by

$$h^m_{u,s} = 10^{\left(\frac{-PL(d) + G_s(\phi) + G_u - \upsilon - \rho}{10}\right)}, \tag{2}$$

where, G_u is the antenna gain, υ is the penetration loss, ρ is the loss due to fading and shadowing, $PL(d)$ is the path loss

TABLE II: Modulation and coding scheme [23].

SINR Threshold (dB)	-6.5	-4	-2.6	-1	1	3	6.6	10	11.4	11.8	13	13.8	15.6	16.8	17.6
Efficiency (bits/symbol)	0.15	0.23	0.38	0.60	0.88	1.18	1.48	1.91	2.41	2.73	3.32	3.9	4.52	5.12	5.55

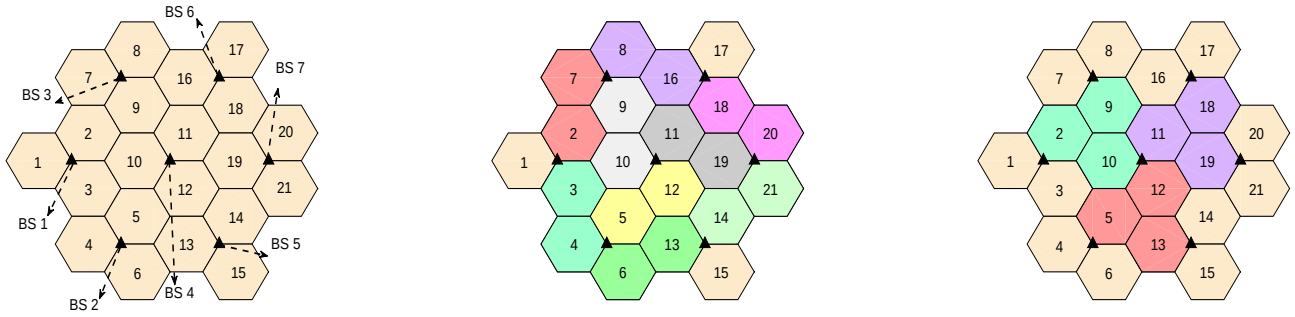

(a) Configuration 1 (C_1) (b) Configuration 2 (C_2) (c) Configuration 3 (C_3)

Fig. 2: Various CoMP configurations for the center cluster.

for the distance d between u and s, and $G_s(\phi)$ is the directivity gain equal to

$$G_s(\phi) = 25 - min\left\{12\left(\frac{\phi}{70}\right)^2, 20\right\}, \forall -\pi \leq \phi \leq \pi, \quad (3)$$

in which ϕ denotes the angle between the u and the main lobe orientation of s [24].

C. Resource Allocation and User Scheduling

Let P_{BS} denote the total transmit power of a BS. Then, given that the BS transmit power is shared among the three sectors of a BS, the power allocated in a sector s per subchannel m, P_s^m, is given by

$$P_s^m = \frac{P_{BS}}{3M}, \quad \forall\ s \in \mathcal{S},\ m \in \mathcal{M}. \quad (4)$$

There exist energy efficient power allocation schemes in the literature [25] which save energy through efficient transmit power allocation. However, it has been shown in [25] that the energy savings through BSS is an order of magnitude higher than energy efficient power allocation schemes. Thus, in this work, we consider uniform power allocation such that the available transmit power per BS is allocated equally among all available subchannels across all the sectors in a BS. This also corresponds to frequency flat fading. The presented analysis can be generalized to frequency selective fading by using water filling based power allocation schemes as discussed in [26].

We use $\eta(\gamma_{u,s}^m)$ to denote the spectral efficiency achieved by a user in bits/symbol. The value of $\eta(\gamma_{u,s}^m)$ obtained from an adaptive modulation and coding scheme (MCS) is given in Table II for various ranges of SINR [23]. Given $\gamma_{u,s}^m$ as in (1), the link rate for the user u from sector s, denoted by $r_{u,s}$, is expressed as

$$r_{u,s} = \frac{\eta(\gamma_{u,s}^m)\, SC_{OFDM}\, SY_{OFDM}}{T_{sc}} M, \quad (5)$$

where, SC_{OFDM}, SY_{OFDM}, and T_{sc} represent the number of subcarriers per subchannel, number of symbols used per subcarrier, and time duration of a subframe, respectively. The factor M represents number of subchannels used in downlink per sector s.

We consider an $\alpha-$Fair time based scheduler at each sector s such that the scheduler allocates all the M subchannels for a downlink time fraction denoted by $\beta_{u,s}$ to a user u associated with it. In the benchmark system, we assume that any user u associates with the sector s from which it receives maximum received SINR on the downlink. Thus, for a user u, $\beta_{u,s}$ is non-zero for only one sector s. The resultant downlink rate for any user u, represented by λ_u, is given by

$$\lambda_u = \sum_{s \in \mathcal{S}} \beta_{u,s} r_{u,s}, \quad (6)$$

where, $r_{u,s}$ is the link rate as computed in (5). The utility function for an α-Fair user scheduler is expressed as [27]

$$\mathbb{U}_\alpha(\lambda) = \begin{cases} \dfrac{\lambda^{1-\alpha}}{1-\alpha}, & \alpha > 0,\ \alpha \neq 1, \\ log(\lambda), & \alpha = 1. \end{cases} \quad (7)$$

To focus on the downlink, we consider the TDD downlink time fraction as 1.

D. CoMP

We consider that the sectors are grouped in pre-determined CoMP clusters such that only sectors from the same CoMP cluster can cooperate and perform CoMP. This is a reasonable assumption as CoMP requires a direct backhaul link between participating sectors. We denote the set of CoMP clusters by $\mathcal{Q} = \{1, 2, ..., Q\}$. Without loss of generality, we focus on the center cluster in Fig. 1 represented by q such that $\mathcal{B}_q$, $\mathcal{W}_q$, and $\mathcal{V}_q$ denote the set of BSs, sectors, and users in the cluster q, respectively. Within the cluster q, several configurations are possible for CoMP based on which sectors perform CoMP together. We represent set of CoMP sectors present in a cluster q as virtual clusters, which is represented by $\mathcal{K}_q = \{1, 2, ..., K\}$. In a virtual cluster k, we use $\mathcal{S}_k$ and $\mathcal{U}_k$ to represent the set

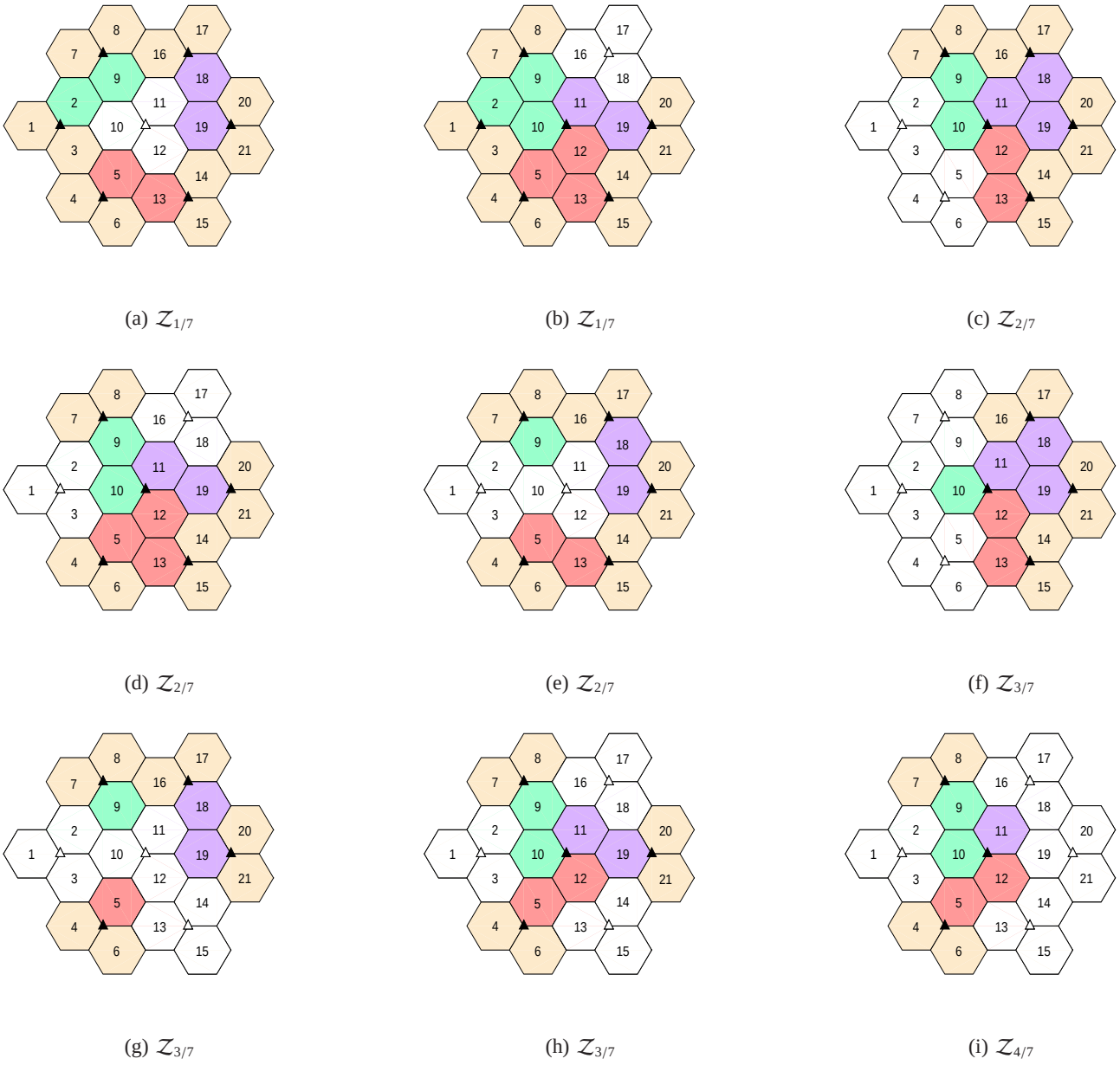

(a) $\mathcal{Z}_{1/7}$ (b) $\mathcal{Z}_{1/7}$ (c) $\mathcal{Z}_{2/7}$

(d) $\mathcal{Z}_{2/7}$ (e) $\mathcal{Z}_{2/7}$ (f) $\mathcal{Z}_{3/7}$

(g) $\mathcal{Z}_{3/7}$ (h) $\mathcal{Z}_{3/7}$ (i) $\mathcal{Z}_{4/7}$

Fig. 3: Various BSS patterns for the center cluster for CoMP configuration 3 (the solid black triangles represent BSs in ON state and white triangles represents BSs that are in OFF state).

of sectors and users, respectively. Thus, a cluster is a group of BSs that performs CoMP, and virtual cluster is the group of sectors within a cluster which performs CoMP. Thus, $\mathcal{S}_k \subseteq \mathcal{W}_q \subset \mathcal{S}$. We consider the following three possible CoMP configurations in the cluster q.

- Configuration 1: In this configuration, also referred to as C_1, as shown in Fig. 2a, a CoMP user in cluster q receive signals jointly from a sectors s of each BS in the cluster q. Thus, the virtual cluster is of size $|\mathcal{W}_q|/3$ for C_1
- Configuration 2: In C_2, at most two sectors coordinate with each other as shown in Fig. 2b. Thus, sectors 1, 15, and 17 do not perform CoMP, while all the other sectors perform CoMP pairwise (sectors with the same colors cooperate).
- Configuration 3: In Fig. 2c, the Configuration 3 or C_3 is presented. The sectors in sets of three namely, {2, 9, 10}, {5, 12, 13}, and {11 ,18, 19} perform CoMP and the other sectors in the cluster q operate without CoMP in C_3.

To focus on other aspects like user scheduling and resource allocation for energy saving we have considered a cluster of 7 BSs and only three CoMP configurations. However, both the cluster size and the CoMP configurations can be adapted for a practical system. The sectors present in any virtual cluster $\mathcal{S}_k$ will vary based on the configuration under consideration as shown in Fig. 2.

We consider that the CoMP based system allocates a fraction of time for CoMP users in which the sectors in the virtual

cluster transmit jointly on the downlink to the CoMP users. Whenever the SINR of a user u associated to a sector s, in the virtual cluster k, is less than a predetermined SINR threshold Γ_d, the user is served as a CoMP user. Let θ_k denote the time fraction in which such CoMP users receive data jointly from their virtual cluster k. During the remaining downlink time fraction $(1-\theta_k)$, each sector transmits to the typical non-CoMP users individually. Note that each virtual cluster k has its own θ_k.

In the CoMP time fraction θ_k, the downlink SINR received by a user u from any virtual cluster k of over subchannel m (denoted by $\gamma^m_{u,k}$) is given by

$$\gamma^m_{u,k} = \frac{\sum\limits_{v\in\mathcal{S}_k} P^m_v h^m_{u,v}}{\sum\limits_{\substack{\hat{v}\in\mathcal{S}\\ \hat{v}\notin\mathcal{S}_k}} P^m_{\hat{v}} h^m_{u,\hat{v}} + \sigma^2}\,, \tag{8}$$

where, $\sum\limits_{v\in\mathcal{S}_k} P^m_v h^m_{u,v}$ is the sum of the received powers for user u from all the sectors in the virtual cluster k and $\sum\limits_{\substack{\hat{v}\in\mathcal{S}\\ \hat{v}\notin\mathcal{S}_k}} P^m_{\hat{v}} h^m_{u,\hat{v}}$ is the interference from all the other sectors in the system which are not part of this virtual cluster k. Note that the SINR for users associated with the non-CoMP sectors and non-CoMP users of CoMP sectors of cluster q will be as in (1). The link rate for a CoMP user u from a virtual cluster k can be obtained using (5) and (8) as

$$r_{u,k} = \frac{\eta(\gamma^m_{u,k})\, SC_{OFDM}\, SY_{OFDM}}{T_{sc}} M\,. \tag{9}$$

Next, we present the various BSS patterns considered in this work.

E. BSS Patterns

Let $\mathcal{Z}_{a1/a2}$ denote a BSS pattern in which a1 out of the total a2 BSs in the cluster are switched off. Hence, if a1 is equal to 0, then all BSs in the cluster are active. In Fig. 3, we depict some of the possible BSS patterns corresponding to $\mathcal{Z}_{1/7}$, $\mathcal{Z}_{2/7}$, $\mathcal{Z}_{3/7}$, and $\mathcal{Z}_{4/7}$ for CoMP configuration C_3. The shaded black triangles represent active BSs and white triangles represent the BSs that have been switched off in Fig. 3. We use idle and active states of the BSs with OFF and ON state interchangeably throughout the text. Note that Fig. 2c represents $\mathcal{Z}_0$ for C_3, where all BSs are active. For a given $a1$ in $\mathcal{Z}_{a1/a2}$, multiple possible BSS patterns exist. For example, Fig. 3a and Fig. 3b are both for $\mathcal{Z}_{1/7}$. Seven such combinations are possible for $\mathcal{Z}_{1/7}$ in which any one of the seven BS in the cluster can be switched off. The proposed optimization problem and the solution heuristic are valid for all such combinations.

F. Performance Metrics

The three key system performance metrics of a cellular network are rate, coverage, and energy. We measure the system performance of user rates through the $\alpha-$Fair throughput obtained over a cluster q as follows [27]

$$\mathcal{T}_\alpha = \begin{cases} \left(\dfrac{1}{|\mathcal{V}_q|}\sum\limits_{u\in\mathcal{V}_q} \lambda_u^{1-\alpha}\right)^{\frac{1}{1-\alpha}}, & \alpha>0,\ \alpha\neq 1\,,\\ \left(\prod\limits_{u\in\mathcal{V}_q}\lambda_u\right)^{\frac{1}{|\mathcal{V}_q|}}, & \alpha = 1\,, \end{cases} \tag{10}$$

where, α is the fairness parameter, λ_u is as defined in (6), and $\mathcal{V}_q$ is the set of users associated with the cluster q.

We define SINR coverage as the probability of a random user u receiving SINR $\gamma^m_{u,s}$ greater than the minimum SINR threshold in Table II from at least one sector s. Further, we define rate coverage as the probability of a random user u receiving rate λ_u greater than the rate threshold R. This rate threshold is a system parameter that can be controlled by the operator.

We consider the percentage of energy saved, represented by $\mathcal{E}$, as the metric for energy efficiency. For a given BSS pattern $\mathcal{Z}_{a1/a2}$ which means $a1$ out of $a2$ BSs are switched off, the percentage energy saving is

$$\mathcal{E} = \frac{a1}{a2}\times 100\,. \tag{11}$$

Next, we consider a snapshot based approach and consider a user realization for a given user density μ. We formulate the joint BSS and CoMP as an optimization problem for this user realization.

III. Joint BSS and CoMP Problem Formulation

We use w_b as a binary BSS variable to denote BS b in ON ($w_b = 0$) or OFF ($w_b = 1$) state. We focus on the cluster q in the center as depicted in Fig. 1. The power consumption of a BS b in idle and active state is given by P_{idle} and P_{tot}, respectively. Then, for a given user realization, to achieve energy efficiency, we should optimize the following objective function [25]

$$\min_{w_b} \sum_{b\in\mathcal{B}_q} w_b P^b_{idle} + (1-w_b)P^b_{tot}\,. \tag{12}$$

The objective function in (12) simplifies to $\min_{w_b} \sum\limits_{b\in\mathcal{B}_q} w_b(P^b_{idle} - P^b_{tot})$. Given P^b_{idle} is always less than P^b_{tot}, for a homogeneous cellular environment, (12) is equivalent to $\max_{w_b} \sum\limits_{b\in\mathcal{B}_q} w_b$. Let $x_{u,s}$ denote an association variable of user u with sector s such that $x_{u,s}\in\{0,1\}$. Then, the BSS with CoMP problem can be framed as an optimization problem for a given user realization as follows.

We consider a maximum SINR based user association and its corresponding binary association variable as $x_{u,s}$. Based on this if any user u is associated to a sector s, this variable $x_{u,s}$ is set to 1, otherwise $x_{u,s}$ is set to 0. We use $z_{u,s}$ as a binary variable that denotes whether the user u associated to sector s will receive CoMP transmission from the virtual cluster k (such that $s\in\mathcal{S}_k$ and $z_{u,s}$=1) or will receive conventional downlink transmission from the sector s ($z_{u,s}$=0). We set the value of $z_{u,s}$ as 1 if the $\gamma^m_{u,s}$ is less than the CoMP SINR threshold Γ_d. Given the number of CoMP and non-CoMP users, the virtual cluster k has to decide the optimal CoMP

time fraction θ_k. We define $\beta_{u,k}$ as the time fraction of θ_k for which an individual CoMP user u receives joint downlink transmission from the virtual cluster k. Further, any user in the center cluster q should obtain a rate higher than a pre-determined rate threshold R with or without CoMP from corresponding virtual cluster k or sector s, respectively. Then, given the utility function in (7), the joint BSS with CoMP resource allocation and user scheduling problem for a cluster q can be formulated as the following optimization problem.

$$\mathbb{B} \quad : \quad \max_{\substack{w_b,\Gamma_d,\beta_{u,k},\\ \beta_{u,s},\theta_k}} \sum_{b\in\mathcal{B}_q} w_b \tag{13}$$

$$\text{s.t.} \quad \sum_{b\in\mathcal{B}_q} w_b \leq |\mathcal{B}_q| - 1\,, \tag{14}$$

$$w_b \in \{0,1\},\ \forall b \in \mathcal{B}_q\,, \tag{15}$$

$$\lambda_u = \Big[\sum_{k\in\mathcal{K}_q}\sum_{s\in\mathcal{S}_k}(1-\theta_k)x_{u,s}(1-z_{u,s})\beta_{u,s}r_{u,s} + \sum_{k\in\mathcal{K}_q}\sum_{s\in\mathcal{S}_k}\theta_k x_{u,s}z_{u,s}\beta_{u,k}r_{u,k}\Big] > R \quad \forall u \in \mathcal{V}_q\,, \tag{16}$$

$$\gamma^m_{u,s} = \frac{(1-w_{\lceil s/3\rceil})P^m_s h^m_{u,s}}{\sum\limits_{\substack{\hat{s}\neq s\\ \hat{s}\in\mathcal{S}}}(1-w_{\lceil \hat{s}/3\rceil})P^m_{\hat{s}}h^m_{u,\hat{s}} + \sigma^2}\,, \tag{17}$$

$$\gamma^m_{u,k} = \frac{\sum\limits_{v\in\mathcal{S}_k}(1-w_{\lceil v/3\rceil})P^m_v h^m_{u,v}}{\sum\limits_{\substack{\hat{v}\in\mathcal{S}\\ \hat{v}\notin\mathcal{S}_k}}(1-w_{\lceil \hat{v}/3\rceil})P^m_{\hat{v}}h^m_{u,\hat{v}} + \sigma^2}\,, \tag{18}$$

$$x_{u,s} = \begin{cases}1, & \text{if } s = \arg\max_s\{\gamma^m_{u,s}\},\\ 0, & \text{otherwise},\end{cases} \forall u \in \mathcal{V}_q, \forall s \in \mathcal{W}_q, \tag{19}$$

$$z_{u,s} = \begin{cases}1, & \text{if } \gamma^m_{u,s} \leq \Gamma_d x_{u,s},\ s\in\mathcal{S}_k,\ k\in\mathcal{K}_q\ s.t.\ |\mathcal{S}_k|>1,\\ 0, & \text{otherwise, } \forall u \in \mathcal{V}_q, \forall s \in \mathcal{W}_q,\end{cases} \tag{20}$$

$$\sum_{s\in\mathcal{S}_k}\ \sum_{u\in\mathcal{U}_k} z_{u,s}x_{u,s}\beta_{u,k} \leq 1,\ \forall k \in \mathcal{K}_q\,, \tag{21}$$

$$\sum_{u\in\mathcal{U}_k} (1-z_{u,s})x_{u,s}\beta_{u,s} \leq 1,\ \forall s \in \mathcal{S}_k,\ \forall k \in \mathcal{K}_q\,, \tag{22}$$

$$\beta_{u,s} \geq 0,\ \forall u \in \mathcal{U}_k,\ \forall s \in \mathcal{S}_k,\ \forall k \in \mathcal{K}_q\,, \tag{23}$$

$$\beta_{u,k} \geq 0,\ \forall u \in \mathcal{U}_k,\ \forall k \in \mathcal{K}_q\,, \tag{24}$$

$$\theta_k \in [0,1],\ \forall k \in \mathcal{K}_q\,, \tag{25}$$

$$\Gamma_d \in [\xi^d_{min}, \xi^d_{max}]\,, \tag{26}$$

where, the objective function in (13) ensures maximum energy savings, while, the constraint in (14) is to ensure that atleast one BS in the center cluster is in ON state, the constraint in (15) reflects that a BS can be either in ON or OFF state, the constraint in (16) is the resultant rate of a user with joint BSS and CoMP, the constraint in (17) is required to account for the change in SINR from a sector with BSS, the SINR from virtual cluster k is recomputed in the constraint in (18) as with BSS the received power from a sector v corresponding to BS $b = \lceil v/3\rceil$ or received power from an interfering sector $\hat{v}$ can be zero if the corresponding BS is switched off, the constraint in (19) is required to re-compute user association with BSS through the additional term of $(1-w_b)$ that ensures the maximum SINR is computed only over the BSs that are still in ON state, the constraint in (20) ensures that a user is served as a CoMP user based on received SINR only from sectors of BSs still in ON state and for virtual cluster with more than one sector available for CoMP, the constraint in (21) indicates that time fractions of θ_k allocated to all CoMP users in cluster k must be less than equal to 1. Similarly, the constraint in (22) indicates that time fractions of $(1-\theta_k)$ allocated individually in each sector s to non-CoMP users must be less than equal to 1. The constraints in (23) and (24) are required to ensure non-negative time fractions for non-CoMP and CoMP users, respectively. The constraint in (25) ensures that the CoMP time fraction is not more than the total available time. The values of ξ^d_{min} and ξ^d_{max} in the constraint (26) define the permitted range for the CoMP threshold Γ_d.

Note that the optimization problem presented in (13) is an MINLP and the problem becomes more complex with increasing number of BSs, i.e., $|\mathcal{B}_q|$. Therefore, we decompose the joint problem of BSS and CoMP in (13) into purely a CoMP resource allocation and user scheduling problem in the next section, and use it to re-frame a simplified BSS with CoMP problem later.

IV. CoMP Problem Formulation

For the CoMP based system, we use $z_{u,s}$, and $x_{u,s}$ as binary variables as explained in the previous section. For a given user realization, this CoMP problem jointly determines the solution for the optimal resource fraction θ_k that can be allocated for CoMP users, the optimal time fraction scheduled for individual users, i.e., $\beta_{u,s}(1-\theta_k)$ fraction of time that can be allocated to a non-CoMP user u by a sector s, and $\beta_{u,k}\theta_k$ fraction of time that can be allocated to a CoMP user jointly from the sectors in the virtual cluster k. Then, given the utility function in (7), the joint CoMP resource allocation and user scheduling problem for a virtual cluster k can be formulated as the following optimization problem.

$$\mathbb{P} \quad : \quad \max_{\substack{\Gamma_d,\theta_k,\\ \beta_{u,s},\beta_{u,k}}} \sum_{u\in\mathcal{U}_k} \mathbb{U}_\alpha(\lambda_u)\,, \tag{27}$$

$$\text{s.t. } \lambda_u = (1-\theta_k)\sum_{s\in S_k} x_{u,s}(1-z_{u,s})\beta_{u,s}r_{u,s} + \theta_k\sum_{s\in S_k} x_{u,s}z_{u,s}\beta_{u,k}r_{u,k}, \quad \forall u \in \mathcal{U}_k\,, \tag{28}$$

$$x_{u,s} = \begin{cases}1, & \text{if } s = \arg\max_s\{\gamma^m_{u,s}\},\\ 0, & \text{otherwise}, \forall u \in \mathcal{U}_k, \forall s \in \mathcal{S}_k\,,\end{cases} \tag{29}$$

$$z_{u,s} = \begin{cases}1, & \text{if } \gamma^m_{u,b} \leq \Gamma_d x_{u,s},\ s\in\mathcal{S}_k\ s.t.\ |\mathcal{S}_k|>1,\\ 0, & \text{otherwise, } \forall u \in \mathcal{U}_k, \forall s \in \mathcal{S}_k\,,\end{cases} \tag{30}$$

$$\sum_{s\in\mathcal{S}_k}\ \sum_{u\in\mathcal{U}_k} z_{u,s}x_{u,s}\beta_{u,k} \leq 1\,, \tag{31}$$

$$\sum_{u\in\mathcal{U}_k} (1-z_{u,s})x_{u,s}\beta_{u,s} \leq 1,\ \forall s \in \mathcal{S}_k\,, \tag{32}$$

$$\beta_{u,s} \geq 0,\ \forall u \in \mathcal{U}_k,\ \forall s \in \mathcal{S}_k\,, \tag{33}$$

$$\beta_{u,k} \geq 0,\ \forall u \in \mathcal{U}_k\,, \tag{34}$$

$$\theta_k \in [0,1]\,, \tag{35}$$

$$(1)\,, (26)\,,$$

where, the user rate is defined by (28) such that any non-CoMP users u gets a fraction of $\beta_{u,s}(1-\theta_k)$ from the sector s and any CoMP users u gets a fraction of $\beta_{u,k}\theta_k$ from all sectors in k, $x_{u,s}$ in (29) represents the maximum SINR based binary user association variable, the constraint in (30) implies that a user can be either CoMP or non-CoMP with corresponding binary $z_{u,s}$. The $r_{u,k}$ in (28) is given in (9).

The joint resource allocation and user scheduling problem in (27) is also an MINLP which is difficult to solve simultaneously for the multiple optimization variables (namely, Γ_d, θ_k, $\beta_{u,s}$, $\beta_{u,k}$). Hence, we next present propositions that provide optimal solutions with respect to $\beta_{u,s}$, $\beta_{u,k}$, and θ_k for a given Γ_d and $x_{u,s}$ in a virtual cluster k. This is a valid assumption as user association ($x_{u,s}$) is typically maximum SINR based and thresholds like Γ_d can be determined via simulations. We first present Proposition 1 which solves the user scheduling problem for any CoMP resource allocation (θ_k) because the user scheduling is independent θ_k.

Proposition 1. *For a virtual cluster k, given a user association $x_{u,s}$, a CoMP SINR threshold Γ_d, at least one CoMP user with $\gamma^m_{u,s} \leq \Gamma_d$, and any CoMP time fraction θ_k, the optimal time fraction of $(1-\theta_k)$, allocated by the α-Fair scheduler in any sector $s \in \mathcal{S}_k$ for a non-CoMP user u is equal to*

$$\beta^*_{u,s} = \frac{\mathtt{t}_{u,s,\alpha}}{\sum\limits_{v\in\mathcal{U}_{nc,s}} \mathtt{t}_{v,s,\alpha}}\ , \forall s \in \mathcal{S}_k,\ \forall u \in \mathcal{U}_{nc}\,, \tag{36}$$

where, $\mathtt{t}_{u,s,\alpha} = r_{u,s}^{\frac{1-\alpha}{\alpha}}$, and the optimal time fraction of θ_k allocated by an α-Fair scheduler for all the sectors jointly to a CoMP user u is equal to

$$\beta^*_{u,k} = \frac{\mathtt{t}_{u,k,\alpha}}{\sum\limits_{v\in\mathcal{U}_c} \mathtt{t}_{v,k,\alpha}},\ \forall u \in \mathcal{U}_c\,, \tag{37}$$

where, $\mathtt{t}_{u,k,\alpha} = r_{u,k}^{\frac{1-\alpha}{\alpha}}$, $\mathcal{U}_c = \{1,2,...U_c\}$, $\mathcal{U}_{nc} = \{1,2,...U_{nc}\}$, and $\mathcal{U}_{nc,s} = \{1,2,...U_{nc,s}\}$ denote the set of CoMP users in $\mathcal{S}_k$, the set of non-CoMP users in $\mathcal{S}_k$, and the set of non-CoMP users in any sector $s \in \mathcal{S}_k$ in the virtual cluster, respectively.

Proof: For any given user association $x_{u,s}$ (note that it need not be maximum SINR based) and CoMP SINR threshold Γ_d, the virtual cluster k can compute $z_{u,s}$ using (30). Given binary $z_{u,s}$, a user u can be classified as CoMP or non-CoMP user into the sets $\mathcal{U}_c$ or $\mathcal{U}_{nc}$, respectively. Further, the set of non-CoMP users for every sector $s \in \mathcal{S}_k$, denoted by $\mathcal{U}_{nc,s}$, can be obtained. Then, as $\mathcal{U}_k = \mathcal{U}_c \cup \mathcal{U}_{nc}$, the objective function in (27) denoted by $\mathbb{Y}$ can be represented as

$$\mathbb{Y} = \sum_{u\in\mathcal{U}_k} \frac{\lambda_u^{1-\alpha}}{1-\alpha} = \sum_{u\in\mathcal{U}_{nc}} \frac{\lambda_u^{1-\alpha}}{1-\alpha} + \sum_{u\in\mathcal{U}_c} \frac{\lambda_u^{1-\alpha}}{1-\alpha}\,, \tag{38}$$

which using (28) becomes

$$\begin{aligned}\mathbb{Y} &= \sum_{u\in\mathcal{U}_{nc}} \sum_{s\in S_k} x_{u,s} \frac{(1-\theta_k)^{1-\alpha}(r_{u,s}\beta_{u,s})^{1-\alpha}}{1-\alpha} \\ &+ \sum_{u\in\mathcal{U}_c} \sum_{s\in S_k} x_{u,s} \frac{\theta_k^{1-\alpha}(r_{u,k}\beta_{u,k})^{1-\alpha}}{1-\alpha}\,.\end{aligned}$$

Then, for any given θ_k, $x_{u,s}$, and Γ_d, the optimization problem in (27) can be simplified to

$$\mathbb{P}^* \quad : \quad \max_{\beta_{u,s}\beta_{u,k}} \ \mathbb{Y} \tag{39}$$

$$\text{s.t.} \quad \sum_{u\in\mathcal{U}_{nc,s}} \beta_{u,s} \leq 1,\ \forall s \in \mathcal{S}_k\,, \tag{40}$$

$$\sum_{u\in\mathcal{U}_c} \beta_{u,k} \leq 1\,, \tag{41}$$

$$(23),\ \text{and}\ (24)\,,$$

where, (40) and (41) are obtained from (21) and (22), respectively. The Lagrangian function of (39) can be defined as

$$\begin{aligned}\mathbf{L}(\mathbb{Y},\mathbb{V}_s,\mathbb{V}_k,\mathbb{X}_{u,s},\mathbb{X}_{u,k}) = -\mathbb{Y} + \sum_{s\in\mathcal{S}_k} \mathbb{V}_s\Big(\sum_{u\in\mathcal{U}_{nc,s}} \beta_{u,s} - 1\Big) + \\ \mathbb{V}_k\Big(\sum_{u\in\mathcal{U}_c} \beta_{u,k} - 1\Big) - \sum_{s\in\mathcal{S}_k}\sum_{u\in\mathcal{U}_{nc,s}} \mathbb{X}_{u,s}\beta_{u,s} - \sum_{u\in\mathcal{U}_c} \mathbb{X}_{u,k}\beta_{u,k}\,,\end{aligned} \tag{42}$$

where, $\mathbb{V}_s$, $\mathbb{V}_k$, $\mathbb{X}_{u,s}$, and $\mathbb{X}_{u,k}$ are the KKT multipliers [28] for (40), (41), (23), and (24), respectively. Considering the complementary slackness KKT conditions, the values of $\mathbb{X}_{u,s}$ and $\mathbb{X}_{u,k}$ turn out to be zero for a user u whenever it receives non-zero $\beta_{u,s}$ or $\beta_{u,k}$ from a sector s or a cluster k, respectively. Thus, the corresponding (42) for users receiving non-zero rate (i.e., $x_{u,s}$=1) becomes

$$\mathbf{L}(\mathbb{Y},\mathbb{V}_s,\mathbb{V}_k) = -\mathbb{Y} + \sum_{s\in\mathcal{S}_k} \mathbb{V}_s\Big(\sum_{u\in\mathcal{U}_{nc,s}} \beta_{u,s} - 1\Big) + \mathbb{V}_k\Big(\sum_{u\in\mathcal{U}_c} \beta_{u,k} - 1\Big)\,. \tag{43}$$

The first-order stationarity conditions of (43) for (40) and (41) result in

$$\frac{d\mathbf{L}}{d\beta_{u,s}} = -\left[(1-\theta_k)r_{u,s}\right]^{1-\alpha}\beta_{u,s}^{-\alpha} + \mathbb{V}_s = 0 \ \text{and} \tag{44}$$

$$\frac{d\mathbf{L}}{d\beta_{u,k}} = -\left[\theta_k r_{u,k}\right]^{1-\alpha}\beta_{u,k}^{-\alpha} + \mathbb{V}_k = 0\,,\ \text{respectively.} \tag{45}$$

Solving (44) and (45) jointly with (40) and (41) result in (36) and (37), respectively. This completes the proof of *Proposition* 1. ■

Note that for $\alpha = 1$, i.e., a proportional fair scheduler, (36) and (37) result in time fractions $1/N_{nc,s}$ and $1/N_c$ for Non-CoMP and CoMP users, respectively, in any sector s of the CoMP cluster. The result presented in (36) and (37) gives the time fraction allocated to the set of users $\mathcal{U}_k$ in the cluster k. It is observed from (36) that the time fraction allocated for a non-CoMP user u depends only on the non-CoMP users in the sector s. Further, (37) presents the time fraction allocated for a CoMP user u in the virtual cluster k which depends on all CoMP users in the same virtual cluster k. Next in Proposition 2, we present optimal resource allocation of CoMP users for the α-Fair scheduler.

Proposition 2. *For a given user association $x_{u,s}$ and CoMP SINR threshold Γ_d, the optimal time fraction θ^*_k for CoMP users in a virtual cluster k is given by*

$$\theta^*_k = \frac{\delta}{1+\delta}\,, \tag{46}$$

TABLE III: Various values of α and corresponding θ_k^* for a virtual cluster k.

α	δ	θ_k^*
1	$\frac{N_c}{N_{nc}}$	$\frac{N_c}{N_c+N_{nc}}$
2	$\sqrt{\left[\frac{\sum_{u\in\mathcal{U}_c}(r_{u,k}\beta_{u,k}^*)^{-1}}{\sum_{u\in\mathcal{U}_{nc}}\sum_{s\in\mathcal{S}_k}x_{u,s}(r_{u,s}\beta_{u,s}^*)^{-1}}\right]}$	$\frac{\delta}{1+\delta}$
α	$\sqrt[\alpha]{\left[\frac{\sum_{u\in\mathcal{U}_c}(r_{u,k}\beta_{u,k}^*)^{1-\alpha}}{\sum_{u\in\mathcal{U}_{nc}}\sum_{s\in\mathcal{S}_k}x_{u,s}(r_{u,s}\beta_{u,s}^*)^{1-\alpha}}\right]}$	$\frac{\delta}{1+\delta}$

where,

$$\delta = \left[\frac{\sum_{u\in\mathcal{U}_c}(r_{u,k}\beta_{u,k}^*)^{1-\alpha}}{\sum_{u\in\mathcal{U}_{nc}}\sum_{s\in\mathcal{S}_k}x_{u,s}(r_{u,s}\beta_{u,s}^*)^{1-\alpha}}\right]^{\frac{1}{\alpha}}, \tag{47}$$

with $\beta_{u,s}^*$ and $\beta_{u,k}^*$ as in (36) and (37), respectively.

Proof: For any given user association $x_{u,s}$ and CoMP SINR threshold Γ_d, the virtual cluster k can be classify users into the sets $\mathcal{U}_c$ or $\mathcal{U}_{nc}$ as shown in the proof of Proposition 1. Then, as $\mathcal{U}_k = \mathcal{U}_c \cup \mathcal{U}_{nc}$, the objective function in (27) can be represented as

$$\sum_{u\in\mathcal{U}_k}\frac{\lambda_u^{1-\alpha}}{1-\alpha} = \sum_{u\in\mathcal{U}_{nc}}\frac{\lambda_u^{1-\alpha}}{1-\alpha} + \sum_{u\in\mathcal{U}_c}\frac{\lambda_u^{1-\alpha}}{1-\alpha},$$

which given $x_{u,s}$ is binary, (28), (36), and (37) becomes

$$\sum_{u\in\mathcal{U}_{nc}}\sum_{s\in\mathcal{S}_k}x_{u,s}\frac{(1-\theta_k)^{1-\alpha}(r_{u,s}\beta_{u,s}^*)^{1-\alpha}}{1-\alpha} + \sum_{u\in\mathcal{U}_c}\frac{\theta_k^{1-\alpha}(r_{u,k}\beta_{u,k}^*)^{1-\alpha}}{1-\alpha}. \tag{48}$$

Differentiating (48) with respect to θ_k and equating to 0 gives

$$(1-\theta_k^*)^{-\alpha}\sum_{u\in\mathcal{U}_{nc}}\sum_{s\in\mathcal{S}_k}x_{u,s}(r_{u,s}\beta_{u,s}^*)^{1-\alpha} = (\theta_k^*)^{-\alpha}\sum_{u\in\mathcal{U}_c}(r_{u,k}\beta_{u,k}^*)^{1-\alpha},$$

which on simplification results in (46). This completes the proof of *Proposition* 2. ∎

The result presented in (46) is valid for any α-Fair scheduler. Further, it is observed from (46) that the optimal time fraction for CoMP users θ_k^* depends on the set of all users $\mathcal{U}_k$ in the virtual cluster k irrespective of whether it is CoMP or non-CoMP. The optimal CoMP time fraction θ_k^* for some commonly used α-Fair schedulers is presented in Table III. Note that for a proportional fair scheduler ($\alpha = 1$), θ_k^* is independent of the user link rates and the time allocated to each user. In Table III, the N_{nc} and N_c in a virtual cluster k are given by

$$N_{nc} = \sum_{s\in\mathcal{S}_k}\sum_{u\in\mathcal{U}_k}(1-z_{u,s})x_{u,s}, \text{ and} \tag{49}$$

$$N_c = \sum_{u\in\mathcal{U}_k}\sum_{s\in\mathcal{S}_k}z_{u,s}x_{u,s}, \text{ respectively.} \tag{50}$$

Next, we present a re-framed and simplified BSS with CoMP optimization problem for the center cluster q.

V. BSS with CoMP

The simplified problem of BSS with CoMP for a given Γ_d, and the optimal $\beta_{u,s}$, $\beta_{u,k}$, and θ_k obtained from (36), (37), and (46), respectively, is formulated as follows

$$\mathbb{B}^* \quad : \quad \max_{w_b}\sum_{b\in\mathcal{B}_q}w_b \tag{51}$$

$$\text{s.t.} \quad (14), (15), (17), (18), (19), (20)$$

$$\lambda_u = \Big[\sum_{k\in\mathcal{K}_q}\sum_{s\in\mathcal{S}_k}(1-\theta_k^*)x_{u,s}(1-z_{u,s})\beta_{u,s}^* r_{u,s} + \sum_{k\in\mathcal{K}_q}\sum_{s\in\mathcal{S}_k}\theta_k^* x_{u,s}z_{u,s}\beta_{u,k}^* r_{u,k}\Big] > R \quad \forall u\in\mathcal{V}_q, \tag{52}$$

$$\beta_{u,s}^* \quad \text{is as in (36)}, \forall u\in\mathcal{V}_q, \ \forall s\in\mathcal{W}_q, \tag{53}$$

$$\beta_{u,k}^* \quad \text{is as in (37)}, \ \forall k\in\mathcal{K}_q, \tag{54}$$

$$\theta_k^* \quad \text{is as in (46)}, \ \forall k\in\mathcal{K}_q, \tag{55}$$

where, the objective function in (51) is the same as in (13), the constraints (14), (15), (17)–(20) are required as in (13). However, (52) which is the resultant rate of a user with BSS and CoMP is now computed using $\beta_{u,s}^*$, $\beta_{u,k}^*$, and θ_k^* from (53), (54), and (55), that are obtained using (36), (37), and (46), respectively. Note that although the optimization problem presented in (51) is relatively simpler than (13), it is still an MINLP. Hence, we next present a heuristic that solves the BSS with CoMP optimization problem.

VI. Proposed Heuristic for BSS with CoMP

In this section, we present a heuristic that selects the optimum BSS pattern for a pre-determined set of virtual clusters that perform CoMP in the center cluster q. The proposed heuristic assumes that the set of users $\mathcal{V}_q$ and the set of received powers for any user u from any sector s, represented by $\{P_s^m h_{u,s}^m\}$ is available. The heuristic considers a set of BSS patterns denoted by $\{\mathcal{Z}_{a1/a2}^j\}$. Note that any element $\mathcal{Z}_{a1/a2}^j$ of this set is equivalent to a unique combination of $\{w_b\}$, the binary BSS indicator variables specified in (15). The heuristic also takes Γ_d and R as an input. The set of BSS patterns is first sorted in an increasing of energy consumption such that any BSS pattern $\{\mathcal{Z}_{a1/a2}^j\}$ consumes less than equal to the energy consumed by $\{\mathcal{Z}_{a1/a2}^{j+1}\}$. The heuristic starts with least energy consuming BSS pattern. Next, the set of received powers $\{P_s^m h_{u,s}^m\}$ is sorted for any user u from all sectors s. Using this operation for every user u, the sector s from which it receives maximum power is identified and $x_{u,s}$ is set as 1. Next, given R it is decided whether a user u is a CoMP or a non-CoMP user. Then, for the BSS pattern under consideration, the received SINRs from the corresponding sector or virtual cluster is computed using (17) or (18), respectively. Note that (17) and (18) consider only the BSs that are still in ON state for the SINR calculations. In a separate loop over the number of users, i.e., $|\mathcal{V}_q|$, the rate of each user is computed. This is required as the user association and SINRs are used to compute the rate of all users in the system as in (16). In case all users receive a rate higher than the rate threshold R then the heuristic stops and selects this BSS pattern as the optimum pattern. Otherwise, the number of switched on BSs is increased and the described steps are repeated for the next BSS pattern. The

Algorithm 1 Dynamic Base Station Switching with CoMP

INPUTS : $\{P_s^m h_{u,s}^m\}$, $\mathcal{V}_q$, Γ_d, R, $\{\mathcal{Z}_{a1/a2}^j\}$
OUTPUTS : $\{\lambda_u\}$, $\mathcal{Z}_{a1/a2}^*$
Sort $\mathcal{Z}_{a1/a2}$ in increasing order of energy consumption
Initialize : $J = |\{\mathcal{Z}_{a1/a2}^j\}|$, j=1
Repeat
Initialize : u=1, $\{z_{u,s}\} = 0$
Repeat
Sort $\{P_s^m h_{u,s}^m\}$ in decreasing order and set $x_{u,s} = 1$
  $\gamma_{u,s} = f(\{P_s^m h_{u,s}^m\})$ as in (17)
if $\gamma_{u,s} \leq \Gamma_d$ **then**
    $\gamma_{u,k} = f(\{P_s^m h_{u,s}^m\})$ as in (18)
  $z_{u,s} = 1$
else
  $z_{u,s} = 0$
end if
  Set $u = u + 1$
Until $u \geq |\mathcal{V}_q| + 1$
Set u=1
Repeat
  Compute λ_u as in (16)
  Set $u = u + 1$
Until $u \geq \mathcal{V}_q + 1$
if $\min\{\lambda_u\} < R$ and $j < J$ **then**
  $j = j + 1$
  Goto Step. 6
else
  $\mathcal{Z}_{a1/a2}^* = \mathcal{Z}_{a1/a2}^j$
  Goto Step. 31
end if
Until $j > J$
Stop

heuristic runs till either a optimum BSS pattern is obtained or all BSs are in ON state. The heuristic is presented as a pseudo-code in Algo. 1.

The practical implementation of the proposed heuristic will run at any one of the BSs in a cluster q, such that this particular BS acts as a centralized controller and takes the decisions for all the BSs in the cluster. Given a user realization, the centralized controller decides whether CoMP should be performed or not based on the operator's rate threshold, and CoMP SINR threshold. The user's information particularly SINR and rate has to be sent to the centralized controller so that it can decide the CoMP configuration, CoMP time fraction, and user scheduling time fractions. This will result in additional overhead on the backhaul which can be compensated in terms of improvement in coverage and energy savings. The computational complexity of the proposed heuristic for every user realization is $O(J(|\mathcal{V}_q||\mathcal{B}_q| + |\mathcal{V}_q|))$. Note that worst case J is equal to $2^{|\mathcal{B}_q|}$. However, in practice, operators can optimize and choose from a lower number of BSS patterns. For example, in the numerical results presented next, we consider J equal to five BSS patterns.

TABLE IV: Simulation Parameters

B	49
Inter-site Distance	500 m
Penetration loss (υ)	20 dB
Loss due to Log-normal shadowing (ρ)	Standard deviation of 8 dB
P_{BS}	46 dBm
σ^2	2.2661e-15
PL(d)	136.8245+(39.086($\log_{10}$d-3)) [24]
M	99
Subchannel Bandwidth	180 KHz
SC_{OFDM}	12
SY_{OFDM}	14
$T_{Subframe}$	1 ms
Cluster size	7

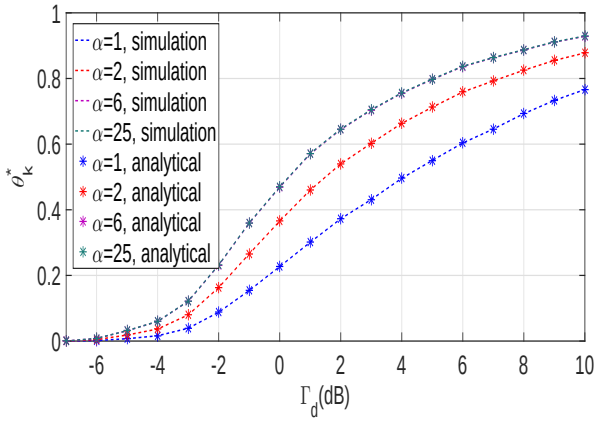

Fig. 4: Variation of optimal CoMP time fraction (θ_k^*) with respect to CoMP SINR threshold (Γ_d) for various fairness parameter (α).

VII. Numerical Results

We consider a center cluster with 7 BSs. To model the interference suitably, we consider a wrap-around system with 6 clusters of 7 BS each around the center cluster. We consider the simulation parameters specified by 3GPP for an urban homogeneous cellular environment as given in [24]. Thus, a total of 49 BSs are considered for simulations with inter-site distance of 500 m. The users are distributed uniformly randomly with the appropriate user density (μ) over the entire simulations area. We consider 500 user location realizations. For each location realization the results are averaged over 50 independent fading realizations. The simulation parameter details are given in Table IV. To study the impact of change in μ over the system performance, we vary the average user density from 20 to 160 users per km^2.

The variation of θ_k^* with respect to Γ_d is shown in Fig. 4 for various values of α. Note that the optimal value of θ_k obtained via exhaustive search in simulations matches with the θ_k^* derived in (46). Further, the optimal CoMP time fraction increases with an increase in the CoMP SINR threshold as more number of users become CoMP users with increase in Γ_d. The increase in α values makes the α-Fair scheduler allocate more resources to edge users. Hence, an increase in the fairness parameter α results in an increase in θ_k^* for the

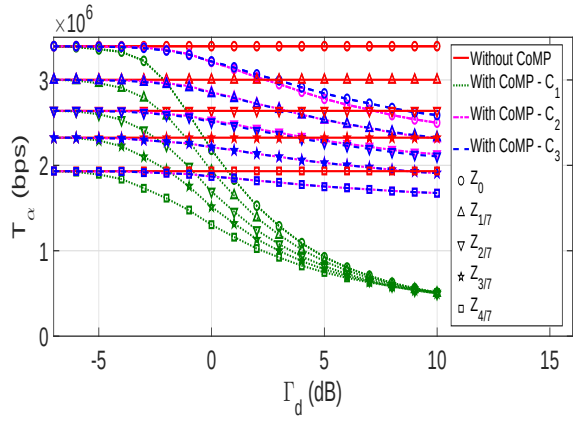

Fig. 5: Variation of system throughput (T_α) with respect to CoMP SINR threshold (Γ_d), with and without CoMP, for various BSS patterns.

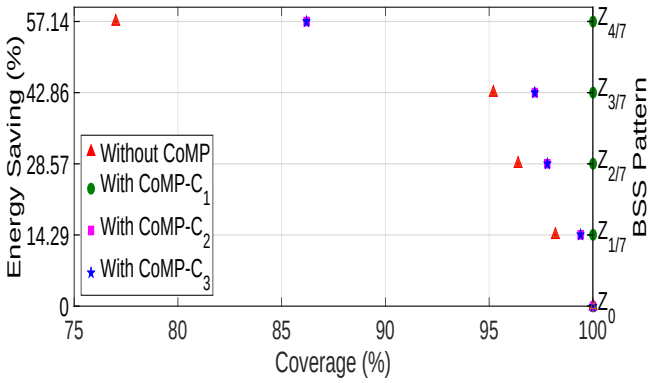

Fig. 7: Energy and coverage trade-off for user density of $60/km^2$, various BSS patterns, and CoMP configurations (Note that the corresponding throughput is depicted in Fig. 8).

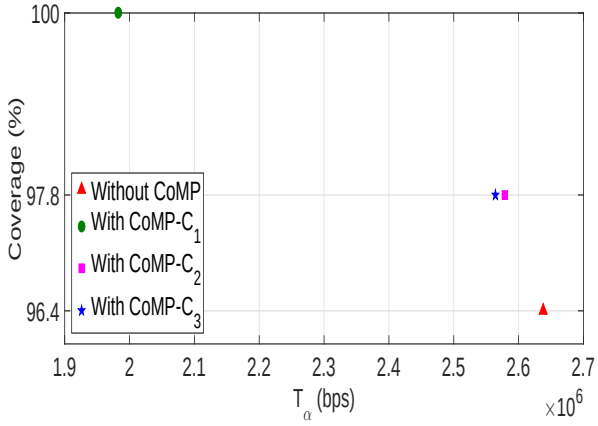

Fig. 6: Coverage and throughput trade-off for user density of $60/km^2$ and BSS pattern $\mathcal{Z}_{3/7}$.

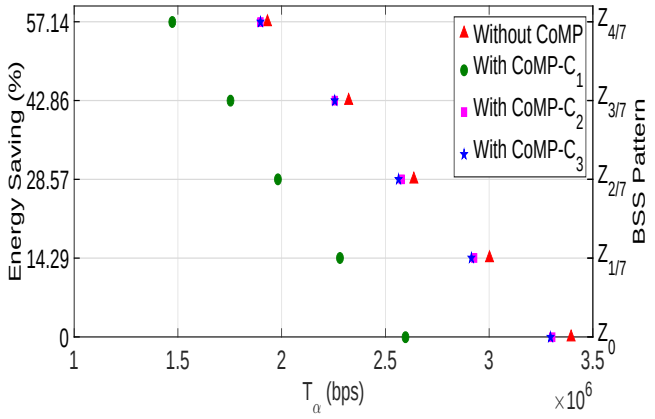

Fig. 8: Energy and throughput trade-off for user density of $60/km^2$, various BSS patterns, and CoMP configurations.

same value of Γ_d. The increased θ_k^* ensures that the edge users (with SINR $\leq \Gamma_d$) will be served as CoMP users and receive more downlink time fraction.

The throughput metric corresponding to a $\alpha-$Fair scheduler is given in (10). The variation of T_α with respect to Γ_d, different BSS patterns, and $\alpha = 1$ is presented in Fig. 5. Note that the throughput decreases as more BSs are switched off. Further, even with various BSS patterns, the without CoMP scenario, CoMP configuration C_3, C_2, and C_1 are in decreasing order of throughput. This is due to the rate and coverage trade-off between these configurations. To better illustrate this, we present the rate and coverage trade-off for the BSS pattern $\mathcal{Z}_{3/7}$ in Fig. 6 for the user density of 60 users/km^2. The probability of coverage is as defined in Section IIF for SINR coverage. Note that an operator can run the network without CoMP for maximum throughput at the cost of coverage. On the other hand, all sectors CoMP in C_1 can provide maximum coverage at the cost of throughput.

The trade-off between percentage energy savings and coverage is presented for $\mathcal{Z}_0$ (all BSs in ON state) and BSS patterns $\mathcal{Z}_{1/7}$, $\mathcal{Z}_{2/7}$, $\mathcal{Z}_{3/7}$ and $\mathcal{Z}_{4/7}$, and various modes of CoMP operations in Fig. 7. The results considered are for BSS patterns shown in Fig. 3b, 3d, 3h, and 3i. An increase in the number of switched off BSs results in decrease in the coverage probability for any particular CoMP configuration. However, switching off BSs also increases the percentage energy savings. Thus, an operator can use the results in 7 to select the appropriate point of operation and the corresponding trade-off between percentage energy savings and coverage.

The corresponding energy and throughput trade-off for the various BSS patterns and CoMP modes in Fig. 7 is presented in Fig. 8. Note that an operator should jointly utilize the Fig. 7 and Fig. 8. For example, in Fig. 7, the coverage probability of C_1 is higher than C_2 for all BSS scenarios. Whereas, in Fig. 8, the throughput of C_1 is lower than C_2 for all BSS scenarios. Thus, multiple configurations of BSS with CoMP can be used to achieve various trade-offs between energy, coverage and rate trade-off which a traditional without CoMP system does not offer.

For the next two set of results, we focus on C_3 as it

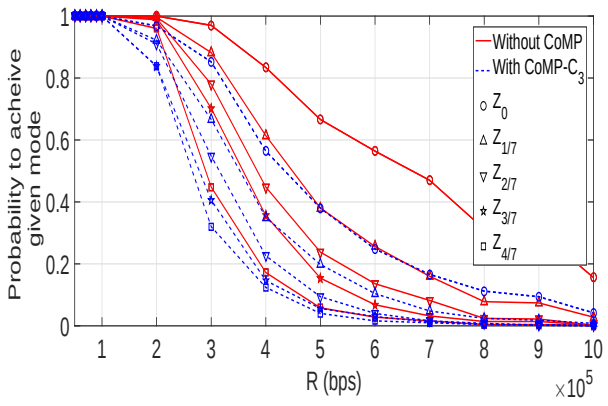

Fig. 9: Variation of rate coverage with respect to rate threshold (R), for various BSS patterns in configuration C_3, $\alpha = 1$, and $\Gamma_d = -1$ dB.

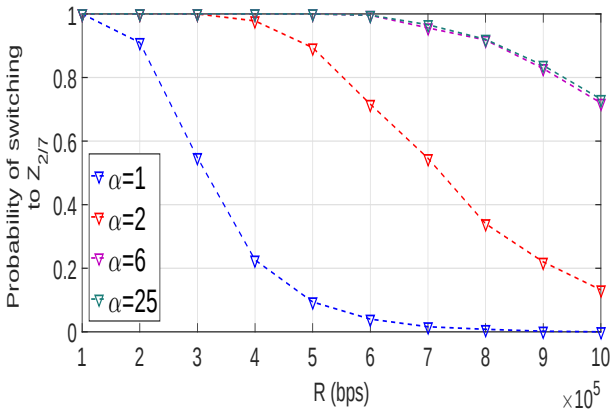

Fig. 10: Variation of rate coverage with respect to rate threshold (R), for various α, BSS pattern $\mathcal{Z}_{2/7}$ in configuration C_3, and $\Gamma_d = -1$ dB.

results in least loss in throughput in comparison to without CoMP scenario. The rate coverage as defined in Section IIF is presented in Fig. 9 and Fig. 10 for $\alpha = 1$ and $\Gamma_d = -1dB$. In Fig. 9, the probability to operate in with a BSS pattern while ensuring the user rates to be higher than the rate threshold R is presented for without CoMP and with CoMP configuration C_3. The Fig. 9 shows that to maintain the same rate coverage with larges energy savings the system has to reduce the rate threshold R. Further, for the same R, BSS patterns with higher energy savings are less probable. Note that Fig. 10 is for BSS pattern $\mathcal{Z}_{2/7}$. It is observed from Fig. 10 that the probability for selecting the BSS pattern increases with increase in α. Thus, Fig. 9 and Fig. 10 also depict the rate-coverage and energy trade-off discussed earlier from a probabilistic perspective.

In Fig. 11, the result from the heuristic proposed in Section VI is presented. We select R as 0.2 Mbps. A snapshot of traffic profile variation is selected and a optimum BSS pattern ($\mathcal{Z}^j_{a1/a2}$) is selected based on the given operator rate threshold R. In Fig. 11, a1 represents the number of BSs switched off and correspondingly the percentage energy saved. It is observed from Fig. 11 that there is some decrease in overall throughput whenever BSs are switched off. However, the loss in throughput is accompanied with significant gain in terms of energy savings. Thus, the proposed heuristic ensures maximum energy savings, without loss in coverage, at the cost of high rate users.

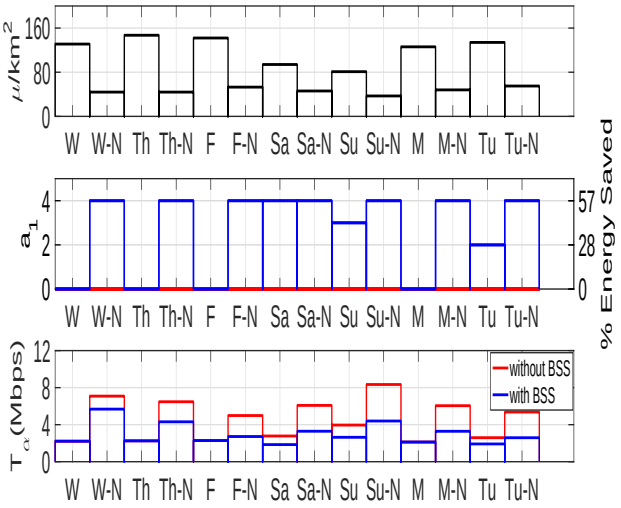

Fig. 11: Performance of the proposed heuristic in a varying traffic scenario when $R = 0.2Mbps$, a1 is number of switched of BSs, μ is user density.

VIII. Conclusion

We have shown that loss in SINR coverage due to BSS can be compensated by CoMP transmission. We have formulated the joint BSS and CoMP problem as an optimization problem. The optimal solutions for a decomposed CoMP resource allocation and user scheduling problem have been derived. The derived results hold for arbitrary BSS patterns, and given a BSS pattern can also be applied to any cluster. The derived results have been used to formulate a simplified BSS with CoMP problem. A heuristic has been presented that solves the BSS with CoMP problem dynamically. Through numerical results it has been shown that the derived results match closely with simulations. Further, we have shown that BSS with CoMP can be used to achieve various possible trade-offs in energy savings, coverage, and throughput. In future, the presented work will be extended using a stochastic geometry based framework for arbitrary cluster size.

References

[1] G. Fettweis and E. Zimmermann, "Ict energy consumption-trends and challenges," in *Proceedings of the 11th International Symposium on Wireless Personal Multimedia Communications*, vol. 2, p. 6, (Lapland, 2008.

[2] J. T. Louhi, "Energy efficiency of modern cellular base stations," in *INTELEC 07-29th International Telecommunications Energy Conference*, 2007.

[3] E. Oh, K. Son, and B. Krishnamachari, "Dynamic base station switching-on/off strategies for green cellular networks," *IEEE transactions on wireless communications*, vol. 12, no. 5, pp. 2126–2136, 2013.

[4] A. Fehske, G. Fettweis, J. Malmodin, and G. Biczok, "The global footprint of mobile communications: The ecological and economic perspective," *IEEE Communications Magazine*, vol. 49, no. 8, pp. 55–62, 2011.

[5] N. Saxena, B. J. Sahu, and Y. S. Han, "Traffic-aware energy optimization in green lte cellular systems," *IEEE Communications Letters*, vol. 18, no. 1, pp. 38–41, 2014.

[6] A. Kumar and C. Rosenberg, "Energy and throughput trade-offs in cellular networks using base station switching," *IEEE Transactions on Mobile Computing*, vol. 15, no. 2, pp. 364–376, 2016.

[7] J. T. Louhi, "Energy efficiency of modern cellular base stations," in *INTELEC 07-29th International Telecommunications Energy Conference*, 2007.

[8] J. Kim, W. S. Jeon, and D. G. Jeong, "Effect of base station-sleeping ratio on energy efficiency in densely deployed femtocell networks," *IEEE Communications Letters*, vol. 19, no. 4, pp. 641–644, 2015.

[9] C. Liu, B. Natarajan, and H. Xia, "Small cell base station sleep strategies for energy efficiency," *IEEE Transactions on Vehicular Technology*, vol. 65, no. 3, pp. 1652–1661, 2016.

[10] Y. L. Che, L. Duan, and R. Zhang, "Dynamic base station operation in large-scale green cellular networks," *IEEE Journal on Selected Areas in Communications*, vol. 34, no. 12, pp. 3127–3141, 2016.

[11] G. R. 151570, "Overview of 3gpp release 12," *3GPP Technical Specification TR*, vol. 36, p. V0.2.0, 2015.

[12] G. Nigam, P. Minero, and M. Haenggi, "Coordinated multipoint joint transmission in heterogeneous networks," *IEEE Transactions on Communications*, vol. 62, no. 11, pp. 4134–4146, 2014.

[13] F. Baccelli and A. Giovanidis, "A stochastic geometry framework for analyzing pairwise-cooperative cellular networks," *IEEE Transactions on Wireless Communications*, vol. 14, no. 2, pp. 794–808, 2015.

[14] X. Ge, H. Jin, J. Cheng, and V. C. Leung, "On fair resource sharing in downlink coordinated multi-point systems,"

[15] S. Y. Park, J. Choi, and D. J. Love, "Multicell cooperative scheduling for two-tier cellular networks," *IEEE Transactions on Communications*, vol. 62, no. 2, pp. 536–551, 2014.

[16] A. He, D. Liu, Y. Chen, and T. Zhang, "Stochastic geometry analysis of energy efficiency in hetnets with combined comp and bs sleeping," in *2014 IEEE 25th Annual International Symposium on Personal, Indoor, and Mobile Radio Communication (PIMRC)*, pp. 1798–1802, IEEE, 2014.

[17] F. Han, Z. Safar, and K. R. Liu, "Energy-efficient base-station cooperative operation with guaranteed qos," *IEEE Transactions on Communications*, vol. 61, no. 8, pp. 3505–3517, 2013.

[18] S. Han, C. Yang, G. Wang, and M. Lei, "On the energy efficiency of base station sleeping with multicell cooperative transmission," in *2011 IEEE 22nd International Symposium on Personal, Indoor and Mobile Radio Communications*, pp. 1536–1540, IEEE, 2011.

[19] K. M. S. Huq, S. Mumtaz, J. Bachmatiuk, J. Rodriguez, X. Wang, and R. L. Aguiar, "Green hetnet comp: Energy efficiency analysis and optimization," *IEEE Transactions on Vehicular Technology*, vol. 64, no. 10, pp. 4670–4683, 2015.

[20] R. Yoghitha and A. Kumar, "Base station switching with comp in cellular networks," in *National Conference on Communication (NCC)*, 2016.

[21] P.-H. Huang, S.-S. Sun, and W. Liao, "Greencomp: Energy-aware cooperation for green cellular networks," *IEEE Transactions on Mobile Computing*, vol. 16, no. 1, pp. 143–157, 2017.

[22] S.-Y. Kim and C.-H. Cho, "Call blocking probability and effective throughput for call admission control of comp joint transmission," *IEEE Transactions on Vehicular Technology*, 2016.

[23] D. López-Pérez, A. Ladanyi, A. Jüttner, H. Rivano, and J. Zhang, "Optimization method for the joint allocation of modulation schemes, coding rates, resource blocks and power in self-organizing lte networks," in *INFOCOM, 2011 Proceedings IEEE*, pp. 111–115, IEEE, 2011.

[24] E. U. T. R. Access, "Further advancements for e-utra physical layer aspects," *3GPP Technical Specification TR*, vol. 36, p. V2, 2010.

[25] J. Wu, Y. Zhang, M. Zukerman, and E. K.-N. Yung, "Energy-efficient base-stations sleep-mode techniques in green cellular networks: A survey," *IEEE Communications Surveys & Tutorials*, vol. 17, no. 2, pp. 803–826, 2015.

[26] D. Tse and P. Viswanath, *Fundamentals of wireless communication*. Cambridge university press, 2005.

[27] J. Ghimire and C. Rosenberg, "Revisiting scheduling in heterogeneous networks when the backhaul is limited," *IEEE Journal on Selected Areas in Communications*, vol. 33, no. 10, pp. 2039–2051, 2015.

[28] S. Boyd and L. Vandenberghe, *Convex optimization*. Cambridge university press, 2004.

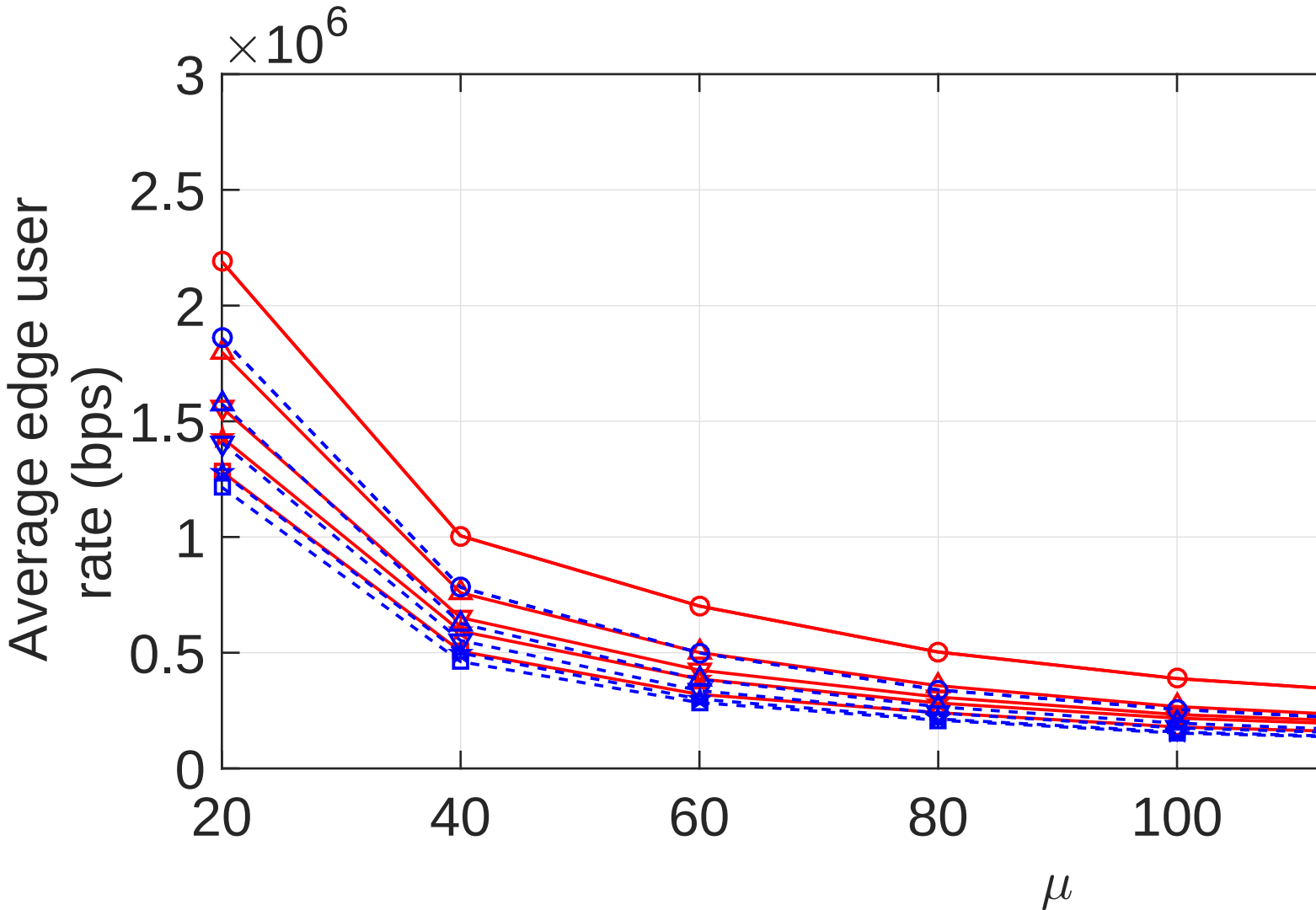
×10^6
3
2.5
2
1.5
1
0.5
0
Average edge user rate (bps)
20
40
60
80
100
μ